

# Novel Lipid Long Intervening Noncoding RNA, Oligodendrocyte Maturation-Associated Long Intergenic Noncoding RNA, Regulates the Liver Steatosis Gene Stearoyl-Coenzyme A Desaturase As an Enhancer RNA

Jihane N. Benhammou,<sup>1-3</sup> Arthur Ko,<sup>4</sup> Marcus Alvarez,<sup>2</sup> Minna U. Kaikkonen,<sup>5</sup> Carl Rankin,<sup>1</sup> Kristina M. Garske,<sup>2</sup> David Padua,<sup>1,3</sup> Yash Bhagat,<sup>2</sup> Dorota Kaminska ,<sup>2,5</sup> Vesa Kärjä,<sup>6</sup> Jussi Pihlajamäki,<sup>5,7</sup> Joseph R. Pisegna,<sup>2,3</sup> and Päivi Pajukanta<sup>2,8,9</sup>

The global obesity epidemic is driving the concomitant rise in nonalcoholic fatty liver disease (NAFLD). To identify new genes involved in central liver functions, we examined liver RNA-sequence data from 259 patients who underwent morbidly obese bariatric surgery. Of these patients, 84 had normal liver histology, 40 simple steatosis, 43 nonalcoholic steatohepatitis, and the remaining 92 patients had varying degrees of NAFLD based on liver histology. We discovered oligodendrocyte maturation-associated long intergenic noncoding RNA (*OLMALINC*), a long intervening noncoding RNA (lincRNA) in a human liver co-expression network ( $n = 75$  genes) that was strongly associated with statin use and serum triglycerides (TGs). *OLMALINC* liver expression was highly correlated with the expression of known cholesterol biosynthesis genes and stearoyl-coenzyme A desaturase (*SCD*). *SCD* is the rate-limiting enzyme in monounsaturated fatty acids and a key TG gene that is known to be up-regulated in liver steatosis and NAFLD and resides adjacent to *OLMALINC* on the human chromosome 10q24.31. Next, we functionally demonstrated that *OLMALINC* regulates *SCD* as an enhancer-RNA (eRNA), thus describing the first lincRNA that functions as an eRNA to regulate lipid metabolism. Specifically, we show that *OLMALINC* promotes liver expression of *SCD* in *cis* through regional chromosomal DNA–DNA looping interactions. **Conclusion:** The primate-specific lincRNA *OLMALINC* is a novel epigenetic regulator of the key TG and NAFLD gene *SCD*. (*Hepatology Communications* 2019;3:1356-1372).

**M**etabolic syndrome (MetS), as defined by the clustering of phenotypic, biochemical, and clinical factors, has reached epidemic proportions in the United States.<sup>(1)</sup> Nonalcoholic fatty liver disease (NAFLD), the liver manifestation of MetS, has also increased in parallel with other

*Abbreviations:* aCRISPR, activating clustered regularly interspaced short palindromic repeats; ASO, antistreptolysin O; cDNA, complementary DNA; ChIP-seq, chromatin immunoprecipitation sequencing; DI, aggregated meta-liver trait; dCas9, dead Cas9; ENCODE, Encyclopedia of DNA Elements; ERCC, External RNA Controls Consortium; eRNA, enhancer RNA; FBS, fetal bovine serum; FDR, false discovery rate; gRNA, guide RNA; GRO-seq, global run-on sequencing; GTEx, genotype-tissue expression; IDT, Integrated DNA Technologies, Inc.; kb, kilobase; KOBAS, Kuopio obesity surgery; LincRNA, long intervening noncoding RNA; LncRNA, long noncoding RNA; LXR, liver X receptor; LXRE, liver X receptor responsive element; MetS, metabolic syndrome; MEM, minimum essential medium; MUFA, monounsaturated fatty acid; NAFLD, nonalcoholic fatty liver disease; NASH, nonalcoholic steatohepatitis; OLMALINC, oligodendrocyte maturation-associated long intergenic noncoding RNA; RNA-seq, RNA sequencing; RT-qPCR, real-time quantitative polymerase chain reaction; SCD, stearoyl-coenzyme A desaturase; siRNA, small interfering RNA; SREBP, sterol regulatory element binding protein; sVA, supervised surrogate variable analysis; TG, triglyceride; TPM, transcript per million; TSS, transcription start site; UCLA, University of California Los Angeles; WGCNA, weighted gene co-expression network analysis; WNT8B, wingless-type MMTV integration site family, member 8B.

Received June 4, 2019; accepted July 10, 2019.

Additional Supporting Information may be found at [onlinelibrary.wiley.com/doi/10.1002/hep4.1413/supinfo](https://onlinelibrary.wiley.com/doi/10.1002/hep4.1413/supinfo).

determinants of MetS.<sup>(2)</sup> NAFLD ranges from simple steatosis to inflammatory nonalcoholic steatohepatitis (NASH), which can lead to fibrosis, cirrhosis, and hepatocellular carcinoma.<sup>(3)</sup> The pathophysiology and interplay of MetS and NAFLD are complex, multifactorial, and include both genetic and environmental contributions.

Intrahepatic lipid accumulation, i.e., steatosis, is the hallmark of NAFLD.<sup>(4,5)</sup> Although the pathogenic pathways that cause progression from steatosis to steatohepatitis and fibrosis remain elusive, human and murine models have demonstrated that lipid dysregulation plays an important role in NAFLD pathogenesis.<sup>(5-8)</sup> Blood lipidomics data in patients with NAFLD<sup>(6,9,10)</sup> and murine knockout models<sup>(11)</sup> have also shown the importance of the monounsaturated fatty acid (MUFA) rate-limiting enzyme stearoyl-coenzyme A desaturase (SCD [also known as SCD-1]), in MetS, steatosis, and NAFLD.<sup>(6,9,10)</sup> Targeting SCD in murine NASH models has shown promising results<sup>(12)</sup> and has recently led to human clinical trials with early phase data demonstrating reversal of

hepatic steatosis using Aramchol, an SCD activity inhibitor.<sup>(13)</sup>

As advances in deep and high-throughput sequencing have emerged, novel players have been identified in lipid biology, including the identification of a unique group of noncoding genes called long noncoding RNAs (lncRNAs).<sup>(14)</sup> LncRNAs are >200 nucleotides long, show tissue and cell-type specificity, and can differentially regulate signaling pathways.<sup>(15)</sup> Understanding their biology has provided insight into new ways in which known key metabolic genes and proteins are regulated beyond previously described mechanisms; such novel ways include acting as scaffolds to complex proteins and enhancer RNAs (eRNAs) and modifying chromatin states.<sup>(14,16)</sup> This has included the role of lncRNAs in the regulation of cholesterol and lipid pathways.<sup>(17)</sup> However, to the best of our knowledge, no eRNA lncRNAs have been discovered to regulate lipid metabolism.

In the present study, we identified the long intervening noncoding RNA (lincRNA) oligodendrocyte

*Supported by the National Institutes of Health (NIH) (grants HL-095056, HL-28481, and DKP3041301 to J.R.P. and P.P.; U01 DK105561 to P.P.; training grant DK007180 to J.N.B.); University of California Los Angeles Specialty Training and Advanced Research Program (to J.N.B.); Howard Hughes Medical Institute Gilliam Fellowship (to M.A.); NIH-National Heart, Lung, and Blood Institute (grant 1F31HL142180 to K.M.G.); Academy of Finland (grants 287478 and 294073 to M.U.K.); Sigrid Jusélius Foundation (to M.U.K.), Finnish Foundation for Cardiovascular Research and European Research Council (Starting Grant 802825 to M.U.K.) and Academy of Finland (grant 316458 to D.K.).*

*The funders had no role in study design, data collection and analysis, decision to publish, or preparation of the article.*

*© 2019 The Authors. Hepatology Communications published by Wiley Periodicals, Inc., on behalf of the American Association for the Study of Liver Diseases. This is an open access article under the terms of the Creative Commons Attribution-NonCommercial-NoDerivs License, which permits use and distribution in any medium, provided the original work is properly cited, the use is non-commercial and no modifications or adaptations are made.*

*View this article online at [wileyonlinelibrary.com](http://wileyonlinelibrary.com).*

*DOI 10.1002/hep4.1413*

*Potential conflict of interest: Nothing to report.*

## ARTICLE INFORMATION:

From the <sup>1</sup>Vatche and Tamar Manoukian Division of Digestive Diseases, University of California Los Angeles, Los Angeles, CA; <sup>2</sup>Department of Human Genetics, David Geffen School of Medicine at University of California Los Angeles, Los Angeles, CA; <sup>3</sup>Division of Gastroenterology, Hepatology, and Parenteral Nutrition, Department of Medicine, Veterans Administration Greater Los Angeles Healthcare System, Los Angeles, CA; <sup>4</sup>Department of Medicine, David Geffen School of Medicine at University of California Los Angeles, Los Angeles, CA; <sup>5</sup>Institute of Public Health and Clinical Nutrition, University of Eastern Finland, Kuopio, Finland; <sup>6</sup>Department of Clinical Pathology, Kuopio University Hospital, Kuopio, Finland; <sup>7</sup>Clinical Nutrition and Obesity Center, Kuopio University Hospital, Kuopio, Finland; <sup>8</sup>Bioinformatics Interdepartmental Program, University of California Los Angeles, Los Angeles, CA; <sup>9</sup>Institute for Precision Health of University of California Los Angeles, Los Angeles, CA.

## ADDRESS CORRESPONDENCE AND REPRINT REQUESTS TO:

Päivi Pajukanta, M.D., Ph.D.  
David Geffen School of Medicine at UCLA  
Gonda Center, Room 6335B  
695 Charles E. Young Drive South

Los Angeles, CA 90095-7088  
E-mail: [ppajukanta@mednet.ucla.edu](mailto:ppajukanta@mednet.ucla.edu)  
Tel.: +1-310-267-2011

maturation-associated long intergenic noncoding RNA (*OLMALINC*) in a statin- and triglyceride (TG)-associated liver co-expression network using liver RNA-sequencing (RNA-seq) from 259 Finnish patients who had undergone bariatric surgery. These patients were from the Kuopio Obesity Surgery (KOBS) cohort and had refined clinical phenotypic and liver histology data. We demonstrate that *OLMALINC* liver expression is highly correlated with the key lipid and TG pathway genes, including *SCD*, in the liver RNA-seq data. We further functionally show that *OLMALINC* regulates this central TG metabolism gene, *SCD*, as a regional eRNA. Taken together, these novel data indicate that *SCD* is regulated by the adjacent lincRNA *OLMALINC*, which likely contributes to the central function of *SCD* in TG metabolism and liver steatosis.

## Participants and Methods

### STUDY COHORTS

The KOBS cohort was recruited at the University of Eastern Finland and Kuopio University Hospital, Kuopio, Finland.<sup>(18)</sup> All participants provided informed consent, and the study was approved by the Ethics Committee of the Kuopio University Hospital, Kuopio, Finland. The liver RNA-seq cohort comprises 259 Finnish KOBS participants who underwent bariatric surgery during which liver biopsies were obtained. Clinical measurements were performed as described.<sup>(18)</sup> We also analyzed liver RNA-seq data on 96 genotype-tissue expression (GTEx) samples.<sup>(19)</sup> We obtained the GTEx data used for the analyses in this manuscript from the GTEx Portal on March 23, 2017.

### HISTOLOGIC ASSESSMENT OF THE LIVER BIOPSY AND META-LIVER TRAIT D1

NASH Clinical Research Network criteria were used to evaluate the liver histologic data.<sup>(20)</sup> The following attributes were used: steatosis grade (0-3), lobular inflammation (0-2), ballooning (0-2), and fibrosis stage (0-4). The diagnosis for NASH was also determined by the pathologist following the standard guidelines.<sup>(21,22)</sup> To determine NAFLD status with liver RNA-seq data, we performed a nonlinear principal component analysis using the homals R package<sup>(23)</sup> on the four Clinical Research

Network liver histologic phenotypes and used the first principal component as the aggregated meta-liver trait (D1) for NAFLD (Fig. 1A). D1 is negatively correlated with the histologic parameters, i.e., a higher D1 represents a healthier liver (Fig. 1A).

### LIVER RNA-seq AND EXPRESSION QUANTIFICATION

RNA samples were isolated using the miRNeasy (Qiagen) kit, and sequencing libraries were prepared using the Ribo-Zero Gold (Illumina) kit to remove ribosomal RNAs. External RNA Controls Consortium (ERCC) spike-ins (Thermo Fisher Scientific) were added as controls. We quantified the transcript abundance as read counts and transcript per million (TPM) using Kallisto<sup>(24)</sup> based on GENCODE version 25 liftover to hg19 gene annotation. Gene-level quantification was estimated as the sums of read counts and TPM of all transcripts of a gene. To remove lowly expressed genes, a gene had to have >10 reads in 80% of samples, resulting in 15,670 genes in the final analysis.

### HIDDEN COVARIATE ESTIMATION FOR RNA-seq

We performed a supervised surrogate variable analysis (sSVA)<sup>(25)</sup> on TPMs and used the 92 ERCC spike-in transcripts as invariable controls to estimate hidden confounders in the liver RNA-seq data. The following covariates were included in the sSVA analysis: uniquely aligned reads %, mitochondrial reads %, 3' bias, body mass index, sex, and age. Overall, 25 latent factors were estimated, and we included all sSVA factors and known covariates in downstream analyses. GTEx data do not contain ERCC spike-ins so we did not carry out sSVA analysis but adjusted for the same covariates as in KOBS.

### STATISTICAL ANALYSIS FOR WEIGHTED GENE CO-EXPRESSION NETWORK ANALYSIS, GENE CORRELATIONS, AND EXPRESSION-TRAIT ASSOCIATIONS

Statistical analyses were performed in R. We transformed raw TPM to  $\log_2(\text{TPM} + 1)$  and then performed empirical Bayes-moderated linear regression

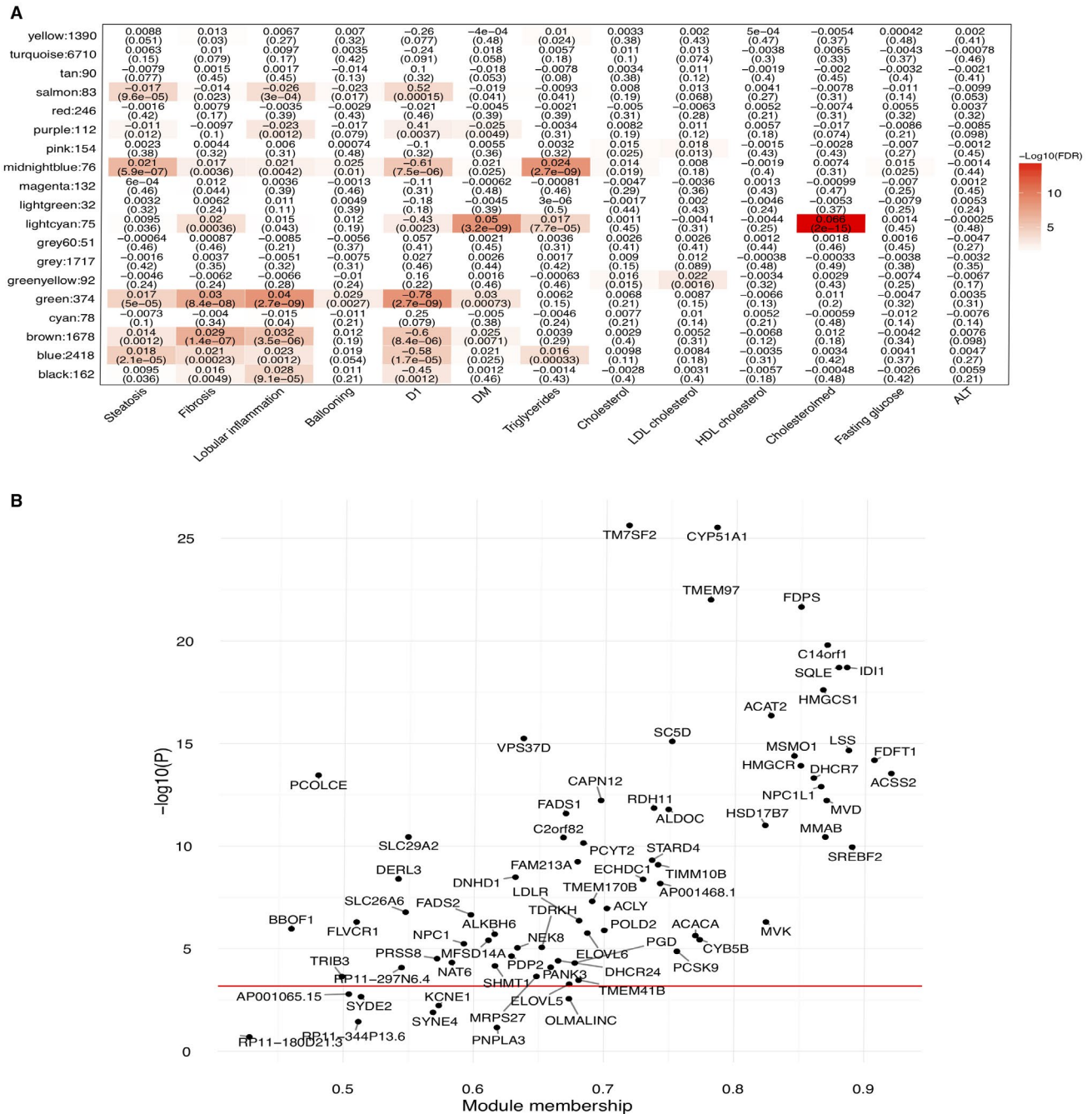


**FIG. 1.** Liver weighted gene co-expression network analyses (WGCNA) identify a statin-associated network module (i.e. the light cyan module). (A) The association results between the liver WGCNA modules and statin use, metabolic traits, and histologic liver phenotypes in the Finnish KOPS cohort. D1 indicates the aggregated meta-liver trait for NAFLD (see Participants and Methods). Numbers in the cells and parentheses indicate effect sizes and FDRs, respectively. (B) Genes in the light cyan module ( $n = 75$ ) are strongly associated with statin medication and involved in cholesterol synthesis. The strength of association with statin medication is highly correlated with the module membership of the light cyan module. The red line indicates the threshold for the Bonferroni-corrected  $P$  value of 0.05. Abbreviations: ALT, alanine aminotransferase; DM, diabetes mellitus; HDL, high-density lipoprotein; LDL, low-density lipoprotein; WGCNA, weighted gene co-expression network analysis.

implemented in the weighted gene co-expression network analysis (WGCNA) package<sup>(26)</sup> (function *empiricalBayesLM*) to correct for covariates while retaining the variation due to the trait of interest. We calculated pairwise gene correlation using biweight correlation allowing a maximum of 5% outliers and

subsequently built a signed network using the soft threshold power of 12. The eigen-gene of each module was calculated and used for trait association tests. To test the module preservation in GTE<sub>x</sub>, we reprocessed the RNA-seq raw reads using our pipeline, the same quality control, and genes expressed in both KOBS and GTE<sub>x</sub>. A module with a preservation summary *Z* statistic >10 was considered as strongly preserved.<sup>(27)</sup> Pairwise gene expression correlation between *OLMALINC* and all other genes was calculated using biweight correlation and the adjusted TPMs. We used linear and logistic regression in all trait association tests, where the adjusted gene expression level and trait were treated as dependent and independent variables, respectively. Quantitative traits were adjusted for age and sex and were inverse normal transformed to avoid outlier effects.

## CELL CULTURE

We maintained HepG2 (American Type Culture Collection, Manassas, VA) and Fa2N4 (XenoTech, Kansas City, Kansas) cells in a monolayer culture at 37°C with 5% CO<sub>2</sub>. The base medium was Eagle's minimum essential medium (MEM) (Corning) for HepG2 and recommended media (XenoTech) containing 100 U/mL penicillin and 100 µg/mL streptomycin sulfate (GE Healthcare Sciences) for Fa2N4. We tested the cells for mycoplasma contamination using the SouthernBiotech Mycoplasma Detection kit.

## REAGENTS AND TRANSFECTIONS

For antistreptolysin O (ASO) treatment, 0.5 million cells were grown to ~70% confluency in six-well plates in triplicates (in 10% fetal bovine serum [FBS] containing 1 g/L glucose with penicillin/ampicillin). Cells were treated with Opti-MEM (Gibco), lipofectamine RNAiMax (13778100; Invitrogen) and ASO (Integrated DNA Technologies, Inc. [IDT]) at a final concentration of 50-100 nM. The control ASO was designed to have similar modifications to the *OLMALINC* ASO. Cells were transfected at a final concentration to 30 pM for small interfering RNAs (siRNAs). ASO and siRNA sequences are provided in Supporting Tables S3 and S4. For plasmid transfections, we used Lipofectamine 3000 (Invitrogen) with 2 µg DNA. For the time-point experiments, cells were incubated overnight in 0.25% bovine serum albumin (Sigma), followed by treatment in corresponding

conditions outlined in the figures.<sup>(28)</sup> We obtained lipoprotein-deficient medium from Kalen Biomedical, LLC; simvastatin sodium salt from Calbiochem dissolved in dimethyl sulfoxide; and GW 3965 and mavelonic acid were kindly provided by Thomas Q de Aguilar Vallim, Department of Biological Chemistry, University of California, Los Angeles, CA. Oleic acid was purchased from Sigma Aldrich. For cellular localization experiments, we used the PARIS kit (Invitrogen). Green fluorescent protein control and *OLMALINC* complementary DNA (cDNA) plasmids were obtained from GeneCopoeia.

## WESTERN BLOTS

Cells were washed and lysed in 1X Laemmli sodium dodecyl sulfate (SDS) sample buffer (Alfa Aesar). Lysates were separated by SDS-polyacrylamide gel electrophoresis (4%-15% polyacrylamide) precast gels (Bio-Rad Laboratories) overnight, transferred to a polyvinylidene difluoride membrane (Immobilon, Millipore Corp.), and blocked for 1 hour in 5% blocking solution (Bio-Rad Laboratories). The membrane was incubated in 1:1,000 primary SCD antibody (Thermo Fisher Scientific) overnight at 4°C, followed by washes in 1:1,000 secondary mouse antibody for 45 minutes. The membrane was washed, after which immunoreactive proteins were detected using chemiluminescence (Bio-Rad Laboratories). Beta-actin (used for the loading control) and secondary mouse antibodies were kindly provided by Dr. Enrique Rozengurt's laboratory (CURE: Digestive Diseases Research Institute, University of California Los Angeles [UCLA], Los Angeles, CA).

## RNA PURIFICATION, cDNA SYNTHESIS, AND REAL-TIME QUANTITATIVE POLYMERASE CHAIN REACTION

We harvested cells in TRIzol (Invitrogen) and extracted their RNA using Direct-Zol (Zymo Research) according to the manufacturer's protocol. We synthesized cDNA using the Maxima First Strand cDNA Synthesis kit (Thermo Scientific). Real-time quantitative polymerase chain reaction (RT-qPCR) was performed using SYBR Green reaction mix (Applied Biosystems) and the Studio 5 detection

system (Applied Biosystems). We used *36B4* as an internal control to normalize the data. The primer list is provided in Supporting Table S2.

## CONSERVATION AND SYNTENY OF *OLMALINC*

To study the conservation of the *OLMALINC* locus, we used the National Center for Biotechnology Information HomoloGene and mouse and human Ensembl data. We evaluated the conservation of *OLMALINC* between human and mouse by aligning DNA segments sequentially between mouse and human using blast (GRCh37/hg19) with the blastn function word size 11, expected threshold 10, match score 2, and mismatch score -3. We also used the mouse Encyclopedia of DNA Elements (ENCODE) data (Mouse mm10) to identify RNA polymerase II and histone methylation markers.

## PROMOTER CAPTURE HI-C

We performed promoter Capture Hi-C in two biological replicates of 10 million HepG2 cells.<sup>(29)</sup> The libraries were sequenced on an Illumina HiSeq 4000 to obtain ~114 million paired-end reads. The reads were processed as described<sup>(30)</sup> using HiCUP<sup>(31)</sup> version 0.7.2 software and aligning to GRCh37/hg19.<sup>(31)</sup> Significant interactions were identified using CHiCAGO software<sup>(32)</sup> version 1.1.1.

## GLOBAL RUN-ON SEQUENCING

Global run-on sequencing (GRO-seq) libraries were prepared according to described protocols in HepG2 cells (10% FBS).<sup>(33,34)</sup> The Illumina HiSeq 2000 platform was used to sequence the libraries after size selection (180-350 base pairs). After quality control, the data were aligned using GRCh37/hg19. GRO-seq data are accessible under Gene Expression Omnibus accession GSE92375.

## ACTIVATING CRISPR DEAD Cas9 STABLE CELL LINES

To generate the activating clustered regularly interspaced short palindromic repeats (aCRISPR) dead Cas9-VP64 (aCRISPR-dCas9) stable cell lines, we used the pHAGE EF10apha dCas9-VP64

(#509181; Addgene) plasmid. Cells were transduced with polybrene (1  $\mu\text{g}/\text{mL}$ ) for 2-3 days, followed by selection with 4  $\mu\text{g}/\text{mL}$  of puromycin for 7 days. Single-clone isolation was obtained following serial dilutions. Clones expressing dCas9 were confirmed by RT-qPCR of the *dCas9* gene. We used two *OLMALINC* guide RNAs (gRNAs) targeting the promoter region of *OLMALINC*.<sup>(35)</sup> gRNAs were obtained from VectorBuilder (Shenandoah, TX).

## CRISPR-Cas9 OF THE *OLMALINC* ENHANCER/PROMOTER REGION

Using IDT Alt-R CRISPR-Cas9 genome editing tools, gRNAs were designed to flank the enhancer/promoter region of *OLMALINC*, which was identified using ENCODE, GRO-seq, and promoter Capture Hi-C. Four gRNAs were used to identify the most efficient gRNAs (Supporting Table S3). RNA protein complexes were prepared using Alt-R S.p. Cas9 Nuclease V3 (IDT) with the *OLMALINC* gRNAs. HepG2 cells were transfected with Opti-MEM (Thermo Fisher Scientific) and Lipofectamine RNAiMax (Invitrogen) for 48 hours. Transfection efficiency was evaluated using light and fluorescent microscopy (Texas Red-X) using the BZ-X710 fluorescent microscope. A FACARIAII cytometer was used to quantify the efficiency of transfection using FACDiva version 8.0.2. We extracted HepG2 genomic DNA using the PureLink Genomic DNA extraction kit (Thermo Fisher Scientific). PCR of the genomic DNA was conducted using primers flanking the gRNA cut sites to detect efficiency of all clones as well as to amplify regions within the *OLMALINC* wild type. These were confirmed using RT-qPCR.

## STATISTICAL METHODS OF THE CELLULAR DATA

For the *in vitro* HepG2 experiments, numeric outcomes are summarized as means  $\pm$  SD or SEM. All relative expression values were measured using  $\Delta\Delta\text{Ct}$ . Experimental groups were compared using the unpaired Student *t* test (for two groups). Analyses were performed using GraphPad Prism version 7.0c. Statistical significance was defined as  $P < 0.05$ . Graphs were made in GraphPad Prism and assembled in Inkspace.

## Results

### IDENTIFICATION OF *OLMALINC* IN THE STATIN- AND TG-ASSOCIATED LIVER CO-EXPRESSION NETWORK

To identify new genes involved in central liver functions, we performed a WGCNA on the liver transcriptomes from 259 participants (40% statin users) in the KOBs surgery cohort and tested the association of co-expression modules with statin use, serum TGs, and other metabolic and liver histology phenotypes measured in this cohort. Thirteen of the 19 co-expression modules were significantly associated (false discovery rate [FDR], <0.05) with at least one of the clinical or histologic traits (Fig. 1A), including the light cyan module (75 genes) that was significantly associated with statin use (FDR,  $2.0 \times 10^{-15}$ ) and serum TGs (FDR,  $7.7 \times 10^{-5}$ ), among other traits (Fig. 1A). We validated the module preservation in an independent human liver RNA-seq cohort, GTEx, by investigating the GTEx subjects whose causes of death were not liver diseases ( $n = 96$ ). Most trait-associated liver modules, such as the statin- and TG-associated light cyan module, were either preserved ( $Z$  score, >3) or highly preserved ( $Z$  score, >10) in the GTEx livers (Supporting Fig. S1), respectively, suggesting that gene coregulation related to main liver functions is robust and consistent across human cohorts. Notably, we observed that the 75 genes in the statin- and TG-associated light cyan network module (Fig. 1A,B) comprise 19 known cholesterol pathway genes, 33 fatty acid and metabolic pathway genes, and several potentially novel statin response and TG genes, including the lincRNA *OLMALINC*. In line with its statin and TG associations, this light cyan module was enriched for the steroid biosynthesis pathway, fatty acid metabolism, and other metabolic pathways (FDR, <0.05) (Supporting Fig. S2), using the Kyoto Encyclopedia of Genes and Genomes pathway database.

Because the lincRNA *OLMALINC* identified in the light cyan module resides immediately downstream from the main TG metabolism gene *SCD* on human chromosome 10 and given that lincRNAs often regulate adjacent coding genes,<sup>(18)</sup> we next individually tested the correlation of *OLMALINC* liver expression with *SCD* and detected a significant correlation

( $\beta = 0.44$ ; FDR,  $4.57 \times 10^{-11}$ ) (Supporting Table S1). We observed that *SCD*, in turn, resides in another WGCNA network, the midnight blue module, that is strongly associated with serum TGs (FDR,  $2.7 \times 10^{-9}$ ) and liver steatosis (FDR,  $5.9 \times 10^{-7}$ ) (Fig. 1A).

Next, we followed up the *OLMALINC* and *SCD* co-expression findings and their mutual associations. We first tested if the liver expression of *OLMALINC* is individually associated with statin usage. When counting for multiple testing of the 75 genes in the light cyan module using Bonferroni (which is a conservative approach because these co-expressed module genes are not entirely independent), *OLMALINC* was nominally associated with statin use ( $P = 0.0035$ ; Fig. 1B). Thus, the statin users appear to have a higher *OLMALINC* liver expression than the non-users in the KOBs cohort; this finding was fully supported by our *in vitro* statin response results in HepG2 cells (see below). Similarly, *SCD* liver expression was also higher in the statin users of the KOBs cohort ( $P = 0.0027$ ), which was again in line with our *in vitro* HepG2 results (see below). We also detected a significant association between *OLMALINC* liver expression and fasting serum TGs in the KOBs cohort ( $\beta = 0.27$ ;  $P = 0.001$ ), passing the Bonferroni correction for six traits (Supporting Table S2). In line with this observation, *SCD* liver expression was significantly associated with serum TGs ( $\beta = 0.48$ ;  $P = 0.13 \times 10^{-7}$ ) in the KOBs cohort as well. Finally, although *OLMALINC* was not associated with steatosis or other liver histology traits (Supporting Table S2), *SCD* liver expression was associated with liver steatosis ( $\beta = 0.35$ ;  $P = 0.0054$ ) but not with NASH ( $\beta = 0.27$ ;  $P = 0.107$ ). Taken together, these novel data suggest the possibility that *OLMALINC* regulates its adjacent regional protein coding gene *SCD*, which is likely the driver in liver steatosis among the two, while both genes are associated with serum TG levels and respond to statin use. To further investigate this new hypothesis that *OLMALINC* regulates *SCD*, we performed functional genomics studies, as described below.

To assess *OLMALINC* gene expression in other human tissues, we analyzed the RNA-seq data from the GTEx project and found that *OLMALINC* is ubiquitously lowly expressed as expected from a lincRNA. After the brain, the most abundant *OLMALINC* expression can be seen in the liver and other endocrine/hormone-regulated organs (Supporting Fig. S3).

## OVERVIEW OF OUR FUNCTIONAL GENOMIC APPROACHES TO STUDY *OLMALINC* IN LIPID METABOLISM

We aimed to study the function of *OLMALINC* by using molecular genomics approaches (Supporting Fig. S4). Because the chromosomal location of *OLMALINC* is directly downstream of *SCD* (see below), we first demonstrated that *OLMALINC* is an enhancer of *SCD* transcription by forming a DNA–DNA looping interaction (Supporting Fig. S4A). This was confirmed by CRISPR–Cas9 genetic deletion of this region (Supporting Fig. S4B) and endogenous transcriptional overexpression using the aCRISPR–dCas9 gene editing system (Supporting Fig. S4D). To complement our CRISPR–Cas9 gene editing, we confirmed that *OLMALINC* positively regulates *SCD* expression (Supporting Fig. S4C) by using an ASO that preferentially localizes to the nucleus. We further showed that *OLMALINC* expression increases with *SCD* siRNA (Supporting Fig. S4E) but decreases with oleic acid treatment, a by-product of *SCD* enzyme activity.

## *OLMALINC* IS STATIN, STEROL, AND LIVER X RECEPTOR RESPONSIVE

Using data from the ENCODE project and chromatin immunoprecipitation sequencing (ChIP-seq) from HepG2 cells, we found two active transcription start sites (TSSs) characterized by an RNA polymerase II binding site, a 5' capped analysis of gene expression (CAGE) peak, and active histone modification markers (characteristic of enhancer and promoter elements) in the *OLMALINC*–*SCD* region (Fig. 2A). GRO-seq data in HepG2 cells, used to assess nascent RNA, not only confirmed two active TSSs in the enhancer and promoter of *OLMALINC* but also demonstrated bidirectional transcription, suggesting that *OLMALINC* could function as an enhancer to *SCD* (Fig. 2A). Using ENCODE project data, we identified sterol regulatory element binding protein (SREBP)1 and SREBP2 ChIP-seq sites at the *OLMALINC* TSSs (Fig. 2B). We hypothesized that *OLMALINC* expression would be statin and sterol responsive, based on our correlative results from the liver RNA-seq data in the KOBS cohort. Using RT-qPCR, we showed

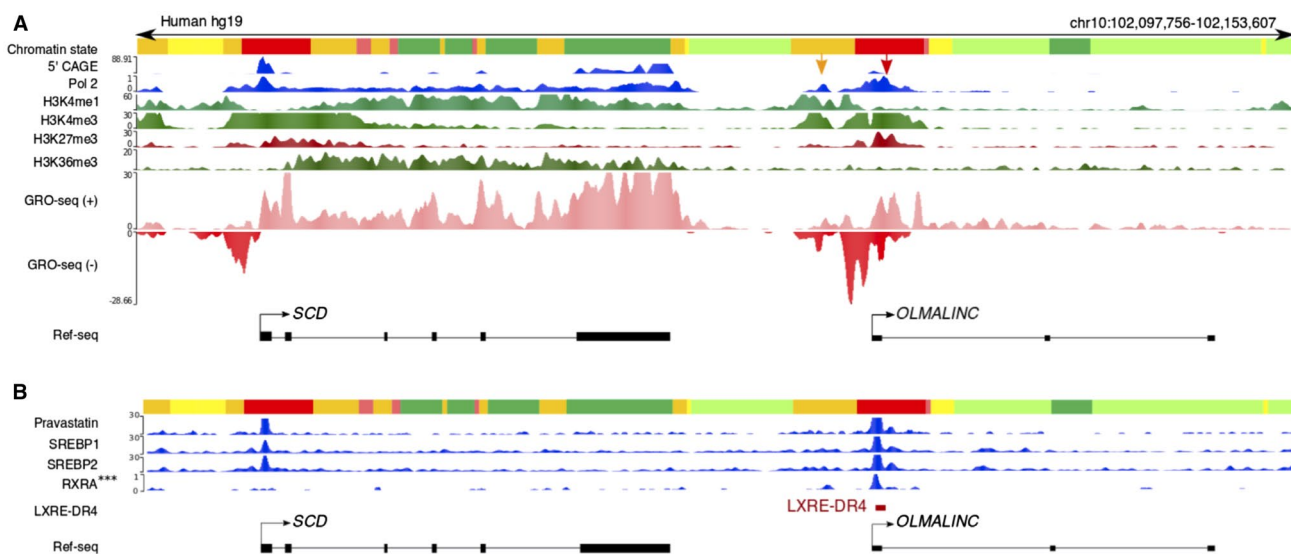


**FIG. 2.** *OLMALINC* resides downstream of *SCD* and demonstrates similar regulatory regions. (A) The annotated *OLMALINC* promoter (red) and enhancer (orange) demonstrate histone methylation marks, 5' CAGE, and polymerase II ChIP-seq binding sites using ENCODE data. There are two TSSs: the orange arrow denotes the enhancer-TSS, while the red arrow highlights the promoter-TSS. Our GRO-seq data in HepG2 cells show active transcription and nascent *OLMALINC* RNA expression bidirectionally. (B) *OLMALINC* has SREBP1/2, pravastatin (pravastatin-treated HepG2 cells with SREBP1/2 peaks), and RXRA binding sites where an LXRE (LXRE-DR4) is identified using sequence comparisons. Abbreviations: CAGE, capped analysis of gene expression; RXRA, retinoid X receptor alpha.

that *OLMALINC* expression increases with statin and sterol treatments in a time-dependent manner, demonstrating that it is both a sterol- and statin-responsive gene (Fig. 3A,B). These data were consistent with the human liver RNA-seq results in the KOBS cohort and demonstrated a positive correlation of *OLMALINC* with liver cholesterol gene expression and a membership in the statin module of our WGCNA analysis (Fig. 1; Supporting Table S1). We also showed that *OLMALINC* expression is liver X receptor (LXR) responsive because cells treated with the synthetic liver LXR $\alpha$  and LXR $\beta$  agonist GW3965 increase *OLMALINC* expression (Fig. 3C). We identified an LXR responsive element (LXRE-DR4) T(G/A) A(C/A) C(T/C) XXXXT(G/A) A(C/A) C(T/C) in the *OLMALINC* promoter (Supporting Fig. S5). This is consistent with *OLMALINC* having a retinoid X receptor alpha ChIP-seq binding site, which forms a heterodimer with LXR $\alpha$  and LXR $\beta$

to activate transcription (Fig. 2B), suggesting a direct role of LXR in regulating *OLMALINC* liver expression. We observed similar data in the immortalized human hepatocyte cell line Fa2N4 when treated with statins and GW3965, thereby corroborating our findings in the HepG2 cell line (Supporting Fig. S6).

## OLMALINC FUNCTION

To study *OLMALINC* function, we analyzed its cellular localization, which did not demonstrate a significant difference between the cytoplasmic and nuclear extracts for exons 1-2 (RT-qPCR of exons 2-3 demonstrated a preferential cytoplasmic expression of the stable transcript) (Supporting Fig. S7B). All subsequent RT-qPCR data that we present were conducted by measuring exons 1-2 (shared between the identified isoforms). A ~50% knock-down of *OLMALINC* by ASO (of exon 2) resulted

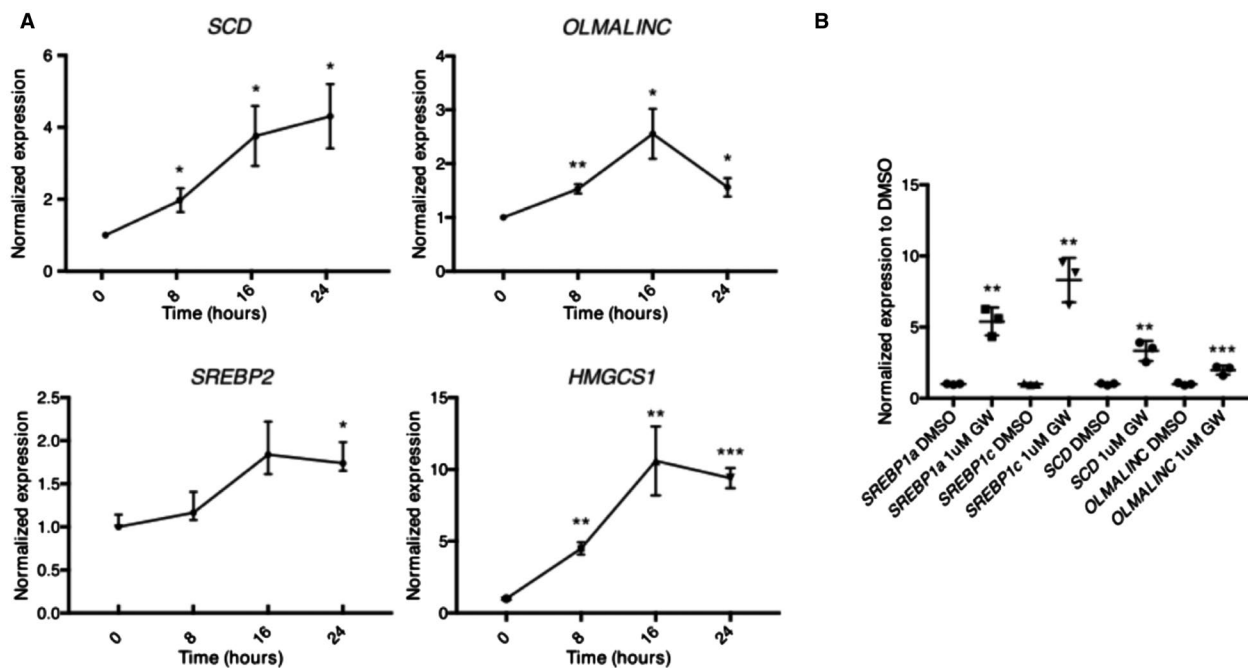


**FIG. 3.** *OLMALINC* expression is responsive to sterols, statins, and LXR agonists in HepG2 cells. (A) *OLMALINC* and *SCD* increase expression by RT-qPCR in a time-dependent manner under sterol-depleted conditions supplemented with statin treatment (5% lipoprotein-deficient media with 5  $\mu$ M simvastatin and 50  $\mu$ M mavelonic acid) when compared to sterol-rich conditions (10% FBS) supplemented with DMSO vehicle control, similarly to *SREBP2* and its downstream gene *HMGCS1*. Each time point was normalized to its DMSO 10% FBS-treated time point. (B) *OLMALINC* gene expression increases after 24-hour treatment of GW3965 (an LXR $\alpha$  and LXR $\beta$  agonist) when compared to the DMSO vehicle control in 5% LPDS with 5  $\mu$ M simvastatin and 50  $\mu$ M mavelonic acid, as measured by RT-qPCR. Values are mean  $\pm$  SD (n = 3) for A and C or mean  $\pm$  SEM for B (n = 3). \* $P$  < 0.05, \*\* $P$  < 0.01, \*\*\* $P$  < 0.001 (unpaired Student  $t$  test was used for two groups). Abbreviations: DMSO, dimethyl sulfoxide; *HMGCS1*, 3-hydroxy-3-methylglutaryl-coenzyme A synthase 1.

in a decrease in *SCD* expression (Fig. 4A; Supporting Fig. S4C). Conversely, when *SCD* was knocked down, we observed an increase in *OLMALINC* expression (Fig. 4B,C). These data suggest that *OLMALINC* expression is responsive to *SCD* expression, its protein level, or the MUFA by-products. Given that *SCD* resides upstream of *OLMALINC* as well as previous observations that lincRNAs can regulate genes in *cis*, we hypothesized that *SCD* is regulated locally by *OLMALINC* in *cis*.

## THE *cis* EFFECTS OF *OLMALINC* ON *SCD* EXPRESSION

*OLMALINC* resides directly downstream of *SCD*, the microsomal enzyme that converts polyunsaturated fatty acids into MUFAs. *OLMALINC* liver expression is significantly correlated with *SCD* expression ( $\beta = 0.44$ ; FDR,  $4.57E-11$ ; Supporting Table S1) and

serum TGs (Supporting Table S2), suggesting a role for *OLMALINC* in TG regulation. The chromosome 10 region of *OLMALINC* and *SCD* in humans has synteny with chromosome 19 of the mouse genome where wingless-type MMTV integration site family, member 8B (*WNT8B*), *SCD1*, *SCD2*, *SCD3*, and *SCD4* are localized in a ~330-kilobase (kb) region (Supporting Fig. S8). However, no orthologues of *OLMALINC* were identified in the mouse. Consistent with these findings, no histone methylation markers or RNA polymerase II ChIP-seq sites were found in the mouse genome between *WNT8B* and *SCD1* to suggest a TSS (Supporting Fig. S9). Similar to other lincRNAs, *OLMALINC* only shows a high homology in primates.<sup>(37)</sup>

Since lincRNAs often exert their function by affecting adjacent genes, we hypothesized that *OLMALINC* may regulate *SCD* expression in *cis* by acting as an enhancer. To further investigate this, we

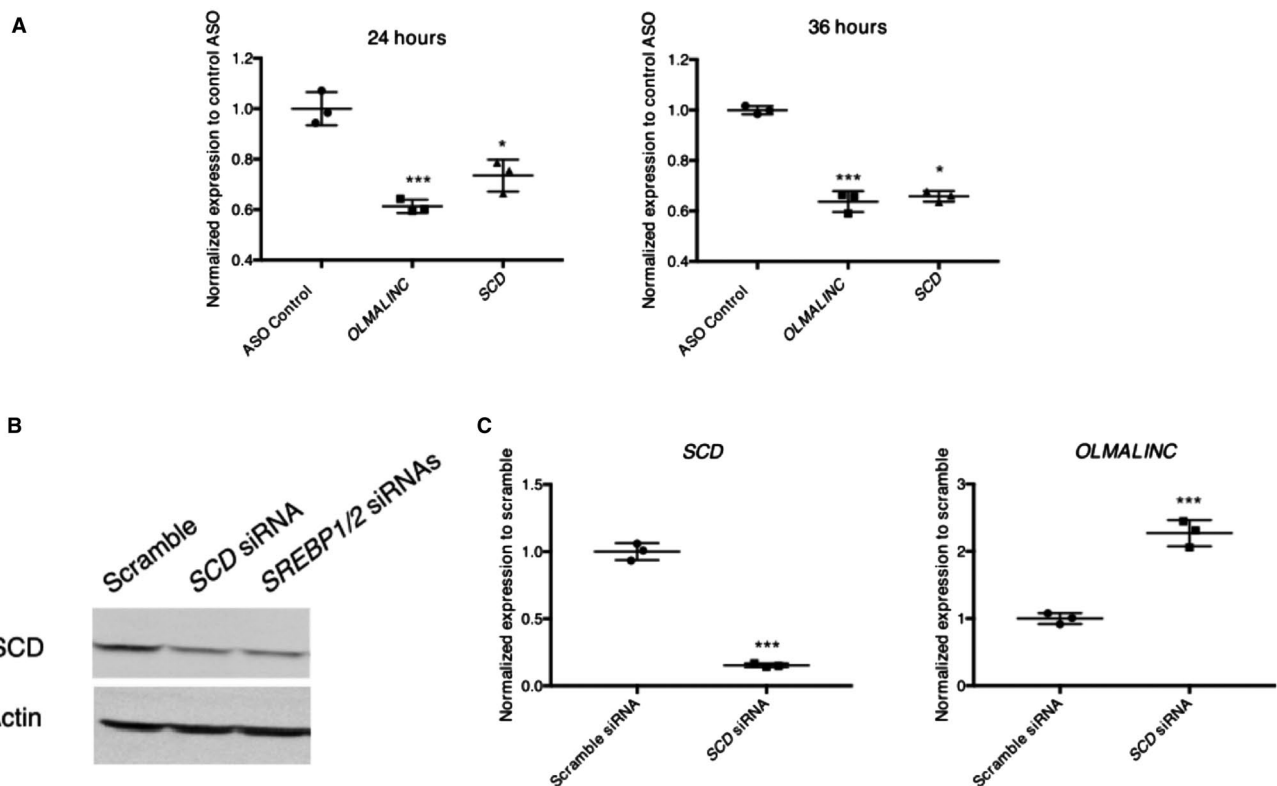


**FIG. 4.** *OLMALINC* ASO introduced to HepG2 cells causes a decrease in expression of *OLMALINC* and target genes. (A) *OLMALINC* and target gene expression, measured by RT-qPCR, decrease after 24-hour and 36-hour treatment with ASO targeting exon 2 of the *OLMALINC* gene. (B) Validation of SCD protein antibody (38 kDa) after treatment with scramble, *SCD*, and *SREBP1* with *SREBP2* siRNAs after 96 hours. (C) *OLMALINC* gene expression increases after 48-hour treatment with an *SCD* siRNA compared to the scramble control. Values are mean  $\pm$  SD ( $n = 3$ ). \* $P < 0.05$ , \*\*\* $P < 0.001$  (unpaired Student  $t$  test was used for two groups).

performed promoter Capture Hi-C in liver HepG2 cells (in 10% FBS) and identified a DNA–DNA looping interaction between the promoter of *SCD* and the annotated promoter/enhancer of *OLMALINC* (Fig. 5A; Supporting Fig. S4A). This interaction is cell-type specific given that no interaction was identified between *SCD* and *OLMALINC* in human adipocytes despite the high *SCD* adipocyte expression.<sup>(29)</sup> These promoter Capture Hi-C interaction data suggest that *OLMALINC* acts by looping in *cis* to affect transcription of *SCD*. It is worth noting that because *OLMALINC* and *SCD* have a bidirectional promoter (Fig. 2B), it is possible that the looping interaction is strand specific; however, only the positive strand was interrogated when targeting the promoter for CRISPR-Cas9 (see below).

To further investigate the *cis* local regulatory effects, we used aCRISPR-dCas9-VP64 to overexpress *OLMALINC* endogenously using previously validated gRNAs in a constitutively expressing dCas9 cell line.<sup>(35,38)</sup> By RT-qPCR, we demonstrated that a ~1.8-fold increase in *OLMALINC* expression resulted

in a 2-fold increase in *SCD* expression (Fig. 5B; Supporting Fig. S4D).

To further tease out the local transcriptional versus posttranscriptional effects of *OLMALINC* regulation, we investigated the effects of its transcript on *SCD* expression. *OLMALINC* is annotated to have several transcripts (data not shown). Expression of a stable transcript with three exons was confirmed by Sanger sequencing of the PCR products (Supporting Fig. S7A) and alignment analysis of the liver RNA-seq (data not shown). When the mature *OLMALINC* transcript is overexpressed using a cDNA construct (exons 1-3), we observed no downstream effects on *SCD* gene expression (Fig. 5C). In conjunction with the endogenous overexpression data (aCRISPR-dCas9), our results confirm that *SCD* regulation by *OLMALINC* occurs at the transcriptional level, likely through the *cis* effects.

To target the *cis* effects of *OLMALINC* on *SCD*, we used CRISPR-Cas9 gene editing to delete the ~3.5-kb region of *OLMALINC*, which encompasses the SREBP1/2 binding sites, TSSs, LXRE, and

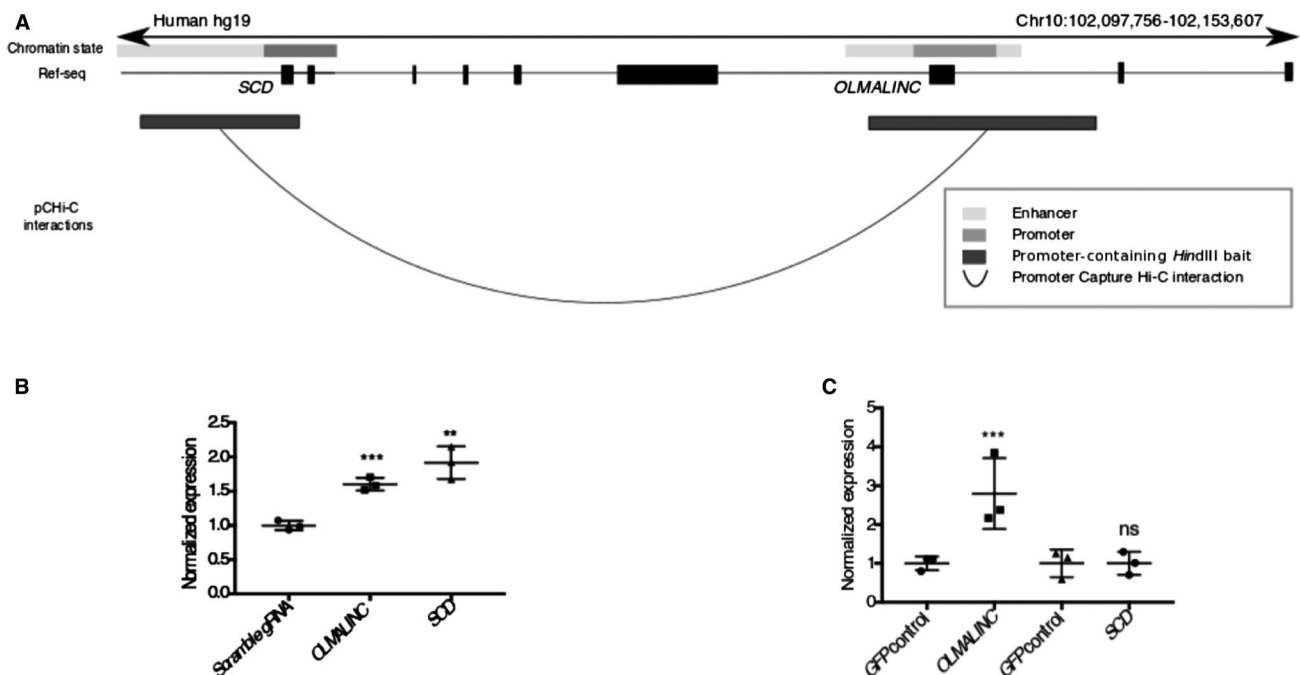


**FIG. 5.** *OLMALINC* regulates *SCD* gene expression in *cis* by forming DNA–DNA looping interactions. (A) Promoter Capture Hi-C data in HepG2 cells demonstrate DNA–DNA looping interactions between the *OLMALINC* enhancer/promoter and the *SCD* promoter/enhancer regions. (B) Endogenous *OLMALINC* overexpression using aCRISPR-dCas9 gene editing increases expression of *SCD*. (C) Overexpression of the spliced *OLMALINC* stable transcript (exons 1-3) for 48 hours does not affect *SCD* gene expression. Expression data are normalized to a GFP negative control. Values are mean  $\pm$  SD ( $n = 3$ ). \*\* $P < 0.01$ , \*\*\* $P < 0.001$  (unpaired Student  $t$  test was used for two groups). Abbreviations: GFP, green fluorescent protein; ns, not significant.

the Capture Hi-C looping interactions (Fig. 6A-C). Using a fluorescently labeled, trans-activating CRISPR RNA (tracrRNA), we determined that our transfection efficiency of the HepG2 cells was 84% (Supporting Fig. S10), thus showing success in targeting the majority of the cells. The cells demonstrate ~50% decrease in *OLMALINC* expression, which causes a decrease in *SCD* expression (Fig. 6D; Supporting Fig. S4B). Whether the *SCD* expression effects are specific to disruption of DNA-DNA interactions between *SCD* and *OLMALINC* encompassing the promoter/enhancer region or are a by-product of large DNA deletions remains to be tested. *Wnt8B*, the gene downstream of *OLMALINC*, is not expressed in human liver, as confirmed by the GTEx cohort and our RT-qPCR data in HepG2 cells (data not shown), thus ruling out a *Wnt8B*-specific effect. Taken together, our detailed functional genomic manipulation of

*OLMALINC* expression (overexpression at the transcriptional level using aCRISPR-dCas9, overexpression posttranscriptionally using the mature cDNA transcript, and knocking down *OLMALINC* RNA by CRISPR-Cas9 and ASO) showed that *OLMALINC* regulates *SCD* expression in *cis* as an enhancer, likely through looping interactions.

## OLMALINC REGULATION

In conjunction with the ENCODE data, we demonstrated that *OLMALINC* is sterol, statin, and LXR responsive (Figs. 2 and 3). Given the *cis* effect of *OLMALINC* on *SCD* and the known regulation of *SCD* by the SREBP1 pathway,<sup>(39)</sup> we sought to further understand *OLMALINC* regulation by these transcription factors. To accomplish this, we knocked down *SREBP1* and *SREBP2* using siRNAs to study

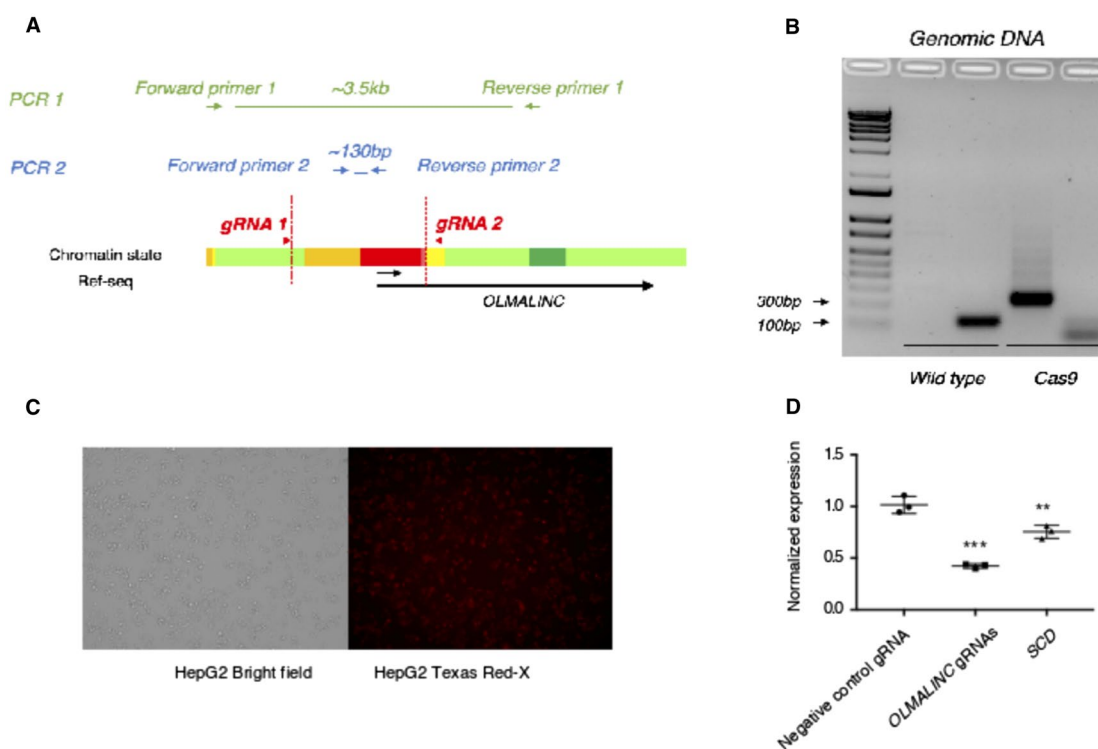


**FIG. 6.** *OLMALINC* enhancer/promoter deletion using CRISPR-Cas9 gene editing decreases *SCD* gene expression. (A) Schematic of primer designs for genomic PCR amplification of wild type versus CRISPR-Cas9-mediated *OLMALINC* promoter/enhancer deletion. Per ENCODE HepG2 chromatin state data, red highlights *OLMALINC* promoter while yellow highlights the enhancer. (B) Gel electrophoresis of PCR products from amplification of the wild type and CRISPR-Cas9 *OLMALINC* enhancer/promoter deletions from the genomic DNA from HepG2 cells. (C) Evaluation of transfection efficiency of HepG2 with fluorescently labeled tracrRNA with ATTO-550 after 24 hours; left panel demonstrating bright field cells and right panel the corresponding labeled cells. (D) *OLMALINC* and *SCD* gene expression by RT-qPCR after 48-hour transfection with the Cas9 enzyme and *OLMALINC* gRNAs flanking the enhancer/promoter region. Values are mean  $\pm$  SD (n = 3). \*\* $P$  < 0.01, \*\*\* $P$  < 0.001 (unpaired Student  $t$  test was used for two groups). Abbreviations: bp, base pair; tracrRNA, trans-activating RNA.

those effects on *OLMALINC* expression. We observed that the knockdown of *SREBP2* or *SREBP1* alone does not affect *OLMALINC* expression or *SREBP1/2*-dependent genes, likely from compensatory effects of the SREBPs (data not shown). However, when both *SREBP1* and *SREBP2* siRNAs are used in conjunction, their target genes, including *SCD*, are decreased while *OLMALINC* expression does not decrease (Fig. 7A). We therefore hypothesized that *OLMALINC* expression is regulated by SCD byproducts, which are MUFAs, possibly through a feedback mechanism. To test this hypothesis, we treated HepG2 cells with the MUFA oleic acid at different time points and demonstrated that *OLMALINC* expression decreases with oleic acid treatment (Fig. 7B), which is consistent with the observed increase in *OLMALINC* expression when knocking down *SCD* (Fig. 4B). We observed that *OLMALINC* gene expression decreases early (18 hours) before seeing an effect on *SCD* gene expression; *SCD* gene expression occurs later at 24 and 48 hours of treatment (Fig. 4B) when we also see a decrease in *SREBP1a* and *SREBP1c*. These data suggest that *OLMALINC* senses and mediates *SCD* gene expression locally before *SREBP1* transcription factor proteins can regulate *SCD* expression. This is in line with our finding that the *OLMALINC* expression is positively correlated only with serum TGs and not with the other phenotypes in the KOBS cohort (Supporting Table S2).

## Discussion

In the present study, we combined human liver transcriptomic and *in vitro* experimental data to identify and characterize the lincRNA *OLMALINC* in lipid metabolism. We first detected *OLMALINC* in tight correlation with known lipid genes in human liver RNA-seq data and then demonstrated that our human correlative expression data translate to important effects of *OLMALINC* on a key TG gene, *SCD*. Our study also describes the first eRNA in lipid metabolism as our data showed that *OLMALINC* regulates the *SCD* gene in *cis*. Specifically, we observed that *OLMALINC* regulates *SCD* at the transcriptional level in *cis* by forming a looping interaction with the *SCD* enhancer/promoter region at important DNA elements where transcription factors and enhancers can interact and activate gene transcription.

Furthermore, as *SCD* encodes an enzyme involved in fatty acid biosynthesis, including the synthesis of the MUFA oleic acid,<sup>(8)</sup> it is noteworthy that in our context-specific lipid-loading experiments, *OLMALINC* expression is responsive to the SCD by-product oleic acid early, independently of *SREBP1*, before seeing changes in *SREBP1a/c*, which occurs later. This suggests that *OLMALINC* may have evolved through an independent mechanism to sense and fine tune *SCD* gene expression early through feedback regulation given its proximity to the gene, perhaps to maintain the important MUFA homeostasis. The underlying molecular mechanism by which oleic acid directly or indirectly regulates *OLMALINC* gene expression warrants further investigation.

Cellular cholesterol and lipid homeostasis are tightly regulated to maintain essential lipid-related processes in the human membrane.<sup>(40)</sup> Important feedback mechanisms are in place to preserve homeostasis at the transcriptional, posttranscriptional, and protein level. This is partly through the SREBP transcription factors, which are the master regulators of cellular lipid and cholesterol processes, with *SREBP1c* preferentially activating the fatty acid synthesis pathway.<sup>(40-42)</sup> Recent studies have demonstrated the role of lincRNAs in regulating and helping regulate SREBPs in their functions.<sup>(14)</sup> For instance, metastasis-associated lung adenocarcinoma transcript 1 (*MALAT1*), the nucleus-specific lincRNA, inhibits degradation of *SREBP1c* protein by preventing its ubiquitination in the nucleus.<sup>(43)</sup> Similarly, the lincRNA *H19* stabilizes *SREBP1c* both at the transcript and protein levels depending if it exerts its function in the cytoplasm or nucleus, respectively.<sup>(44)</sup> In this study, we demonstrate that *OLMALINC* acts as an enhancer for *SCD* and regulates *SCD* expression through sensing of its by-products before *SREBP1*-dependent effects.

Patients with NASH and NAFLD have previously been shown to exhibit altered cholesterol and TG metabolism.<sup>(6,9)</sup> Because the majority of the participants in the KOBS cohort have some form of NAFLD, it is possible that the statin-associated co-expression module we identified in the WGCNA analysis may also reflect the primary effect that NAFLD and NASH have on cholesterol metabolism. However, the correlative WGCNA data cannot alone separate these two possibilities. As *SCD* has been shown to be dysregulated in NAFLD and NASH,<sup>(5,6,9)</sup> future studies are warranted to elucidate the role of *OLMALINC*

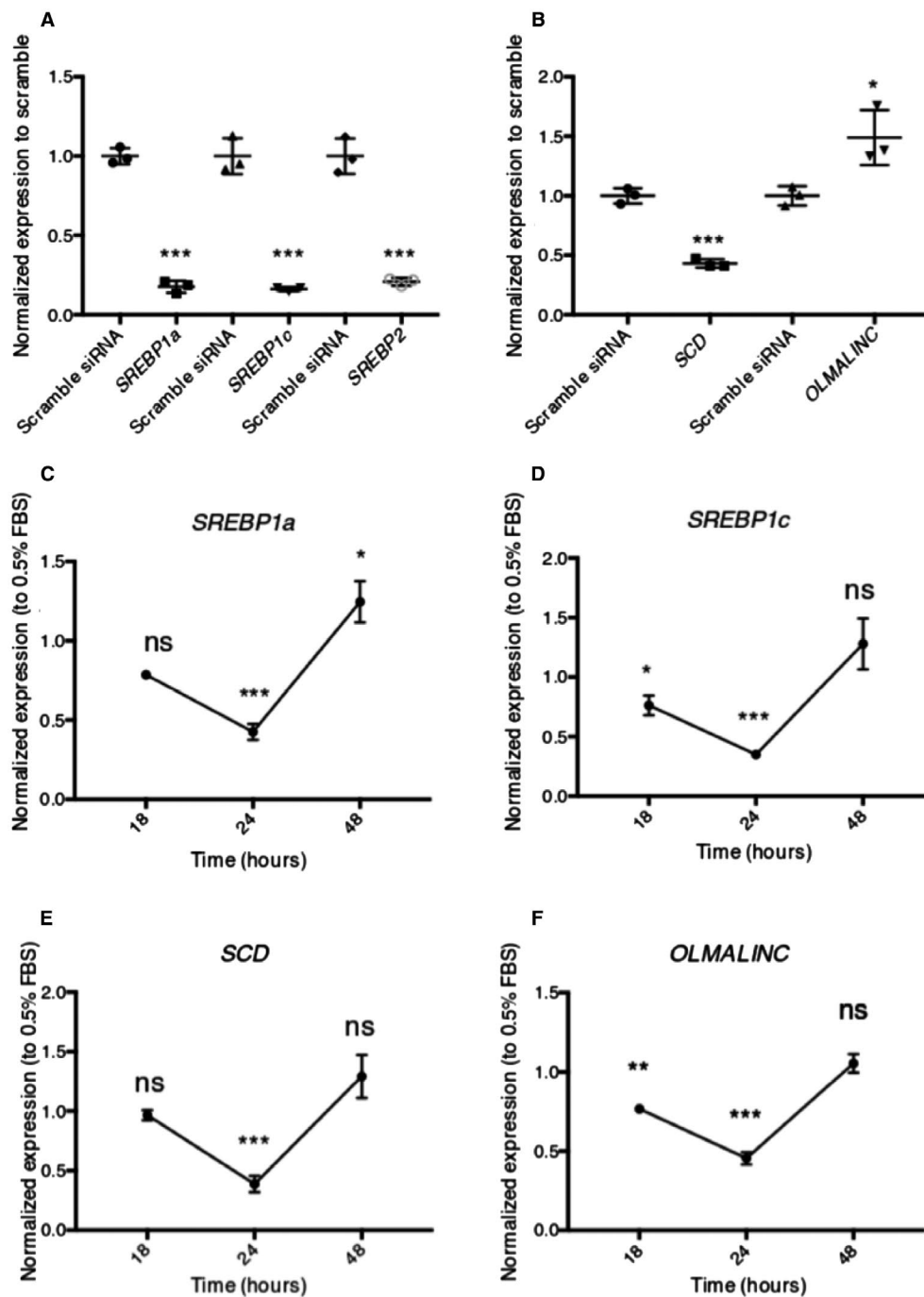


**FIG. 7.** *OLMALINC* is regulated by MUFAs but not by *SREBP1/2*. (A) *SREBP1a*, *SREBP1c*, and *SREBP2* gene expression after *SREBP1* and *SREBP2* siRNA cotransfection for 48 hours, relative to scramble siRNA control. (B) *OLMALINC* expression does not decrease after a 48-hour cotransfection with *SREBP1* and *SREBP2* siRNAs; *SCD* decreases. (C-E) *SREBP1a*, *SREBP1c*, and *SCD* expression decreases after lipid loading with MUFAs (200  $\mu$ M oleic acid) 24-hour treatment only, following 8 hours of starvation in 0.5% FBS. (F) *OLMALINC* decreases its expression after lipid loading with MUFAs (200  $\mu$ M oleic acid) after 18-hour and 24-hour treatment, following 8 hours of starvation in 0.5% FBS. All expression time points are normalized to the corresponding gene expression in 0.5% FBS. Values are mean  $\pm$  SD ( $n = 3$ ). \* $P < 0.05$ , \*\* $P < 0.01$ , \*\*\* $P < 0.001$  (unpaired Student  $t$  test was used for two groups).

in cholesterol metabolism. Because *OLMALINC* expression was not correlated with the liver phenotypes of steatosis and NASH in the KOBS cohort, it is unlikely to play a direct role in the pathophysiology of NAFLD and/or NASH. Future liver lipidomic studies could potentially provide further evidence of how this novel lincRNA affects or is affected by liver-specific lipids. However, some of its specific lincRNA characteristics would have to be taken into account in future studies of *OLMALINC*. We demonstrate that *OLMALINC* regulates *SCD* as an enhancer RNA locally through chromosomal looping interactions (Fig. 5) and early by responding to oleic acid (Fig. 7C-F); given these local and early changes, it may be challenging to measure lipid changes using the current ASO and CRISPR methods because transfection protocols require longer time courses for sufficient knockdown and knockout, respectively. As *OLMALINC* is a primate-specific lincRNA<sup>(35)</sup> (Supporting Figs. S7 and S8), the value of *in vivo* rodent models will also likely be somewhat limited.

Recent studies have demonstrated that lincRNAs affect nearby coding gene expression similarly to the effects of *OLMALINC* on *SCD* expression.<sup>(45)</sup> Through detailed transcriptional analyses, it has also been elucidated that the effects on the nearby genes by lincRNAs are not necessarily mediated through the transcript but rather by transcriptional regulation (through enhancers and promoters) and/or splicing machinery.<sup>(16)</sup> In addition to the important enhancer/promoter region through which *OLMALINC* affects *SCD*, we show that *OLMALINC* has a stable, spliced, and polyadenylated transcript. Given that enhancers generally produce unstable transcripts without a poly-A tail or splicing,<sup>(46)</sup> *OLMALINC* likely has a secondary function on other targets independently of its *cis* effects on *SCD* expression; this function remains to be elucidated.

Consistent with the importance of SCD in metabolic disorders, patients with NASH demonstrate increased *SCD* expression in the liver.<sup>(9)</sup> Plasma oleate to stearate (18:1/18:0) and palmitoleate to palmitate (16:1/16:0) ratios, which are used as surrogates for systemic *SCD* activity, are also increased in patients with MetS and NASH, supporting an increase in SCD activity.<sup>(10)</sup> These data are corroborated by recent clinical trials targeting SCD protein in patients with NASH (n = 58) and human immunodeficiency virus (who also develop hepatic steatosis; n = 25), which

demonstrates reversal of hepatic steatosis with treatment.<sup>(13,47)</sup> In agreement with the human data, *SCD*<sup>-/-</sup> mouse models are protected from adiposity, have decreased *de novo* lipogenesis, and have increased fatty acid oxidation.<sup>(11)</sup> It has also been shown that repletion of oleate through dietary supplementation in global and liver-specific *SCD* knockout murine models prevents hepatic endoplasmic reticulum stress and inflammation.<sup>(48)</sup> Given these findings, it would not be surprising for a lincRNA to have evolved to maintain MUFA homeostasis and provide another layer of early regional regulation to *SCD* gene expression epigenetically through chromosomal looping of this adjacent coding gene. Although far from therapeutic considerations, further understanding of *OLMALINC* function opens up unexplored avenues for gene modification and treatment considering its cell and tissue specificity.

The present study highlights a novel lincRNA, *OLMALINC*, that affects a key TG gene by affecting *SCD* expression in *cis* as a regional eRNA. *OLMALINC* joins a group of lipid lincRNAs that have been described and continue to emerge in lipid homeostasis and pathology.<sup>(17)</sup> In addition to their role in regulating important coding genes, they could be one of many factors that explain the cross-species differences in lipid metabolism. Further unraveling of their biology will provide insight into new cellular mechanisms and may pave the way for better understanding of complex cardiometabolic disorders in humans.

*Acknowledgment:* We thank the participants of the KOBS and GTEx cohorts. We also thank the sequencing core at UCLA for performing the liver RNA-seq; the EMBL GeneCore Sequencing Facility ([https://www.embl.de/services/core\\_facilities/genecore/index.html](https://www.embl.de/services/core_facilities/genecore/index.html)) for GRO-seq; and the UCLA flow cytometry core for cell sorting. We thank the UCLA Integrated Molecular Technologies Core (CURE/P30 DK041301), Dr. Enrique Rozengurt and Jim Sinnet-Smith for their help with western blotting, and Dr. Gregory Brent and Dr. Thomas Q. de Aguiar Vallim for their feedback. GTEx was supported by the Common Fund of the Office of the Director of the National Institutes of Health and by the National Cancer Institute, National Human Genome Research Institute, National Heart, Lung, and Blood Institute, National Institute on Drug Abuse, National Institute of Mental Health, and National Institute of Neurological Disorders and Stroke.

## REFERENCES

- 1) Vernon G, Baranova A, Younossi ZM. Systematic review: the epidemiology and natural history of non-alcoholic fatty liver disease and non-alcoholic steatohepatitis in adults. *Aliment Pharmacol Ther* 2011;34:274-285.
- 2) Younossi ZM, Koenig AB, Abdelatif D, Fazel Y, Henry L, Wymer M. Global epidemiology of nonalcoholic fatty liver disease—meta-analytic assessment of prevalence, incidence, and outcomes. *Hepatology* 2016;64:73-84.
- 3) Brunt EM, Tiniakos DG. Histopathology of nonalcoholic fatty liver disease. *World J Gastroenterol* 2010;16:5286-5296.
- 4) Browning JD, Horton JD. Molecular mediators of hepatic steatosis and liver injury. *J Clin Invest* 2004;114:147-152.
- 5) Min HK, Kapoor A, Fuchs M, Mirshahi F, Zhou H, Maher J, et al. Increased hepatic synthesis and dysregulation of cholesterol metabolism is associated with the severity of nonalcoholic fatty liver disease. *Cell Metab* 2012;15:665-674.
- 6) Chiappini F, Coilly A, Kadar H, Gual P, Tran A, Desterke C, et al. Metabolism dysregulation induces a specific lipid signature of nonalcoholic steatohepatitis in patients. *Sci Rep* 2017;7:46658.
- 7) Mannisto VT, Simonen M, Soininen P, Tiainen M, Kangas AJ, Kaminska D, et al. Lipoprotein subclass metabolism in nonalcoholic steatohepatitis. *J Lipid Res* 2014;55:2676-2684.
- 8) Ntambi JM. Regulation of stearoyl-CoA desaturase by polyunsaturated fatty acids and cholesterol. *J Lipid Res* 1999;40:1549-1558.
- 9) Walle P, Takkunen M, Mannisto V, Vaitinen M, Lankinen M, Kärjä V, et al. Fatty acid metabolism is altered in non-alcoholic steatohepatitis independent of obesity. *Metabolism* 2016;65:655-666.
- 10) Puri P, Wiest MM, Cheung O, Mirshahi F, Sargeant C, Min HK, et al. The plasma lipidomic signature of nonalcoholic steatohepatitis. *Hepatology* 2009;50:1827-1838.
- 11) Ntambi JM, Miyazaki M, Stoehr JP, Lan H, Kendziorski CM, Yandell BS, et al. Loss of stearoyl-CoA desaturase-1 function protects mice against adiposity. *Proc Natl Acad Sci U S A* 2002;99:11482-11486.
- 12) Iruarrizaga-Lejarreta M, Varela-Rey M, Fernandez-Ramos D, Martínez-Arranz I, Delgado TC, Simon J, et al. Role of Aramchol in steatohepatitis and fibrosis in mice. *Hepatol Commun* 2017;1:911-927.
- 13) Safadi R, Konikoff FM, Mahamid M, Zelber-Sagi S, Halpern M, Gilat T, et al.; FLORA Group. The fatty acid-bile acid conjugate Aramchol reduces liver fat content in patients with nonalcoholic fatty liver disease. *Clin Gastroenterol Hepatol* 2014;12:2085-2091.e2081.
- 14) van Solingen C, Scacalossi KR, Moore KJ. Long noncoding RNAs in lipid metabolism. *Curr Opin Lipidol* 2018;29:224-232.
- 15) Kopp F, Mendell JT. Functional classification and experimental dissection of long noncoding RNAs. *Cell* 2018;172:393-407.
- 16) Kaikkonen MU, Adelman K. Emerging roles of non-coding RNA transcription. *Trends Biochem Sci* 2018;43:654-667.
- 17) Sallam T, Jones MC, Gilliland T, Zhang L, Wu X, Eskin A, et al. Feedback modulation of cholesterol metabolism by the lipid-responsive non-coding RNA LeXis. *Nature* 2016;534:124-128.
- 18) Mannisto VT, Simonen M, Hyysalo J, Soininen P, Kangas AJ, Kaminska D, et al. Ketone body production is differentially altered in steatosis and non-alcoholic steatohepatitis in obese humans. *Liver Int* 2015;35:1853-1861.
- 19) GTEx Consortium. The Genotype-Tissue Expression (GTEx) project. *Nat Genet* 2013;45:580-585.
- 20) Kleiner DE, Brunt EM, Van Natta M, Behling C, Contos MJ, Cummings OW, et al.; Nonalcoholic Steatohepatitis Clinical Research Network. Design and validation of a histological scoring system for nonalcoholic fatty liver disease. *Hepatology* 2005;41:1313-1321.
- 21) Brunt EM. Histopathology of non-alcoholic fatty liver disease. *Clin Liver Dis* 2009;13:533-544.
- 22) Simonen M, Mannisto V, Leppanen J, Kaminska D, Kärjä V, Venesmaa S, et al. Desmosterol in human nonalcoholic steatohepatitis. *Hepatology* 2013;58:976-982.
- 23) de Leeuw J, Mair P. Gifi methods for optimal scaling in R: the package homals. *J Stat Softw* 2009;31:1-21.
- 24) Bray NL, Pimentel H, Melsted P, Pachter L. Near-optimal probabilistic RNA-seq quantification. *Nat Biotechnol* 2016;34:525-527. Erratum in: *Nat Biotechnol* 2016;34:888.
- 25) Leek JT. svaseq: removing batch effects and other unwanted noise from sequencing data. *Nucleic Acids Res* 2014;42:e161.
- 26) Langfelder P, Horvath S. WGCNA: an R package for weighted correlation network analysis. *BMC Bioinformatics* 2008;9:559.
- 27) Langfelder P, Luo R, Oldham MC, Horvath S. Is my network module preserved and reproducible? *PLoS Comput Biol* 2011;7:e1001057.
- 28) Tarling EJ, Edwards PA. ATP binding cassette transporter G1 (ABCG1) is an intracellular sterol transporter. *Proc Natl Acad Sci U S A* 2011;108:19719-19724.
- 29) Mijsud B, Tavares-Cadete F, Young AN, Sugar R, Schoenfelder S, Ferreira L, et al. Mapping long-range promoter contacts in human cells with high-resolution Capture Hi-C. *Nat Genet* 2015;47:598-606.
- 30) Wingett S, Ewels P, Furlan-Magaril M, Nagano T, Schoenfelder S, Fraser P, et al. HiCUP: pipeline for mapping and processing Hi-C data. *F1000Res* 2015;4:1310.
- 31) Cairns J, Freire-Pritchett P, Wingett SW, Várnai C, Dimond A, Plagnol V, et al. CHiCAGO: robust detection of DNA looping interactions in Capture Hi-C data. *Genome Biol* 2016;17:127.
- 32) Wang D, Garcia-Bassets I, Benner C, Li W, Su X, Zhou Y, et al. Reprogramming transcription by distinct classes of enhancers functionally defined by eRNA. *Nature* 2011;474:390-394.
- 33) Kaikkonen MU, Niskanen H, Romanoski CE, Kansanen E, Kivelä AM, Laitalainen J, et al. Control of VEGF-A transcriptional programs by pausing and genomic compartmentalization. *Nucleic Acids Res* 2014;42:12570-12584.
- 34) Engreitz JM, Haines JE, Perez EM, Munson G, Chen J, Kane M, et al. Local regulation of gene expression by lncRNA promoters, transcription and splicing. *Nature* 2016;539:452-455.
- 35) Mills JD, Kavanagh T, Kim WS, Chen BJ, Waters PD, Halliday GM, et al. High expression of long intervening non-coding RNA OLMALINC in the human cortical white matter is associated with regulation of oligodendrocyte maturation. *Mol Brain* 2015;8:2.
- 36) Pan DZ, Garske KM, Alvarez M, Bhagat YV, Boock J, Nikkola E, et al. Integration of human adipocyte chromosomal interactions with adipose gene expression prioritizes obesity-related genes from GWAS. *Nat Commun* 2018;9:1512. Erratum in: *Nat Commun* 2018;9:3472.
- 37) Konermann S, Brigham MD, Trevino AE, Joung J, Abudayyeh OO, Barcena C, et al. Genome-scale transcriptional activation by an engineered CRISPR-Cas9 complex. *Nature* 2015;517:583-588.
- 38) Liu SJ, Horlbeck MA, Cho SW, Birk HS, Malatesta M, He D, et al. CRISPRi-based genome-scale identification of functional long noncoding RNA loci in human cells. *Science* 2017;355:1-9.
- 39) Shimano H, Horton JD, Shimomura I, Hammer RE, Brown MS, Goldstein JL. Isoform 1c of sterol regulatory element binding protein is less active than isoform 1a in livers of transgenic mice and in cultured cells. *J Clin Invest* 1997;99:846-854.
- 40) Shimano H, Shimomura I, Hammer RE, Herz J, Goldstein JL, Brown MS, et al. Elevated levels of SREBP-2 and cholesterol

- synthesis in livers of mice homozygous for a targeted disruption of the SREBP-1 gene. *J Clin Invest* 1997;100:2115-2124.
- 41) Brown MS, Goldstein JL. The SREBP pathway: regulation of cholesterol metabolism by proteolysis of a membrane-bound transcription factor. *Cell* 1997;89:331-340.
  - 42) Horton JD, Goldstein JL, Brown MS. SREBPs: activators of the complete program of cholesterol and fatty acid synthesis in the liver. *J Clin Invest* 2002;109:1125-1131.
  - 43) Yan C, Chen J, Chen N. Long noncoding RNA MALAT1 promotes hepatic steatosis and insulin resistance by increasing nuclear SREBP-1c protein stability. *Sci Rep* 2016;6:22640.
  - 44) Liu C, Yang Z, Wu J, Zhang L, Lee S, Shin DJ, et al. Long noncoding RNA H19 interacts with polypyrimidine tract-binding protein 1 to reprogram hepatic lipid homeostasis. *Hepatology* 2018;67:1768-1783.
  - 45) Ebisuya M, Yamamoto T, Nakajima M, Nishida E. Ripples from neighbouring transcription. *Nat Cell Biol* 2008;10:1106-1113.
  - 46) Kim TK, Shiekhatter R. Architectural and functional commonalities between enhancers and promoters. *Cell* 2015;162:948-959.
  - 47) Ajmera VH, Cachay E, Ramers C, Vodkin I, Bassirian S, Singh S, et al. MRI assessment of treatment response in HIV-associated NAFLD: a randomized trial of a stearoyl-coenzyme-A-desaturase-1 inhibitor inhibitor (ARRIVE Trial). *Hepatology* 2019. <https://doi.org/10.1002/hep.30674>.
  - 48) Liu X, Burhans MS, Flowers MT, Ntambi JM. Hepatic oleate regulates liver stress response partially through PGC-1alpha during high-carbohydrate feeding. *J Hepatol* 2016;65:103-112.

Author names in bold designate shared co-first authorship.

## Supporting Information

Additional Supporting Information may be found at [onlinelibrary.wiley.com/doi/10.1002/hep4.1413/supinfo](http://onlinelibrary.wiley.com/doi/10.1002/hep4.1413/supinfo).